A short-term regional precipitation prediction model based on wind-improved spatiotemporal convolutional network

Yunan Qiu[a], Zhenyu Lu[b], and Haibo Tang[b]

[a]School of Electronics and Information Engineering, Nanjing University of Information Science and Technology, Nanjing, China
[b]School of Artificial Intelligence, Nanjing University of Information Science and Technology, Nanjing, China

Key Points:

- Meteorological data are processed to build a dataset for automatic stations in Jiangsu province.
- The improved GCN takes into account the effects of the wind direction at past moments and geographical location to capture the spatial correlation.
- The proposed model is more in line with the physical characteristics of precipitation and suitable for precipitation prediction tasks.

Corresponding author: Yunan Qiu, 20201118008@nuist.edu.cn

Abstract

Accurate precipitation forecasting can better reflect climate change trends, provide timely and effective environmental information for management decisions, and prevent flood and drought disasters. In this paper, we propose a short-term regional precipitation prediction model based on wind-improved spatiotemporal convolutional network. Among them, the improved Graph Convolution Network (GCN) integrates the effects of wind direction and geographic location at past moments to capture the spatial dependence, whilst the Gated Recurrent Unit (GRU) captures the temporal dependence by learning the dynamic changes of data. The spatio-temporal memory flow module and attention module are added to capture spatial deformation and temporal variation more accurately, thereby better matching the physical properties of precipitation. Experimental results on real data sets show that the proposed model can handle complex spatial dependence and temporal dynamic changes, better learn the temporal and spatial characteristics of precipitation data, and achieve better prediction results.

Plain Language Summary

Deep learning technology has not been fully explored in regional short-term precipitation prediction. The traditional graph convolution neural network does not consider the practical significance of wind direction in precipitation. Therefore, we introduce a novel short-term regional precipitation prediction model based on wind improved spatiotemporal convolution network (ASS-TGCN). Measured data of automatic meteorological station in Jiangsu Province, China have been utilized. The experimental results show that the prediction result of the proposed model is better than the comparative model and has higher prediction accuracy.

1 Introduction

Regional precipitation, as a vital component of the hydrological system, plays a critical role in the entire water cycle(Hawkins & Sutton, 2011). The rapid changes in regional precipitation that occur in a short period of time often cause severe droughts and floods, seriously impacting the national economy. Short-term heavy precipitation refers to precipitation events with rainfall of more than 20 mm within 1 hour or 50 mm within 3 hours (Ban et al., 2015). This kind of weather process presents the characteristics of fierce rain, high precipitation intensity within a short amount of time and high disaster risk. As such, it can easily cause urban and rural waterlogging and traffic congestion. Furthermore, in mountainous areas, it is easy to lead to landslides, flash floods, debris flows, and other disasters(Henderson et al., 2020), that seriously threaten the safety of people's lives and property(Yao et al., 2021). In light of such endangerment, proximity precipitation forecasting not only improves the capability of emergency response in dealing with sudden disasters, but also provides a good warning and guide for environmental protection and agricultural production.However, precipitation prediction has proven difficult due to its variability is often complex, variable, and uncertain; it is influenced by environmental factors such as local topography, climate, atmospheric circulation, ocean currents, sunspots, and human activities (Zhang et al., 2018), in addition to possessing complex spatial and time-dependent properties. Of note, learning the higher order properties of spatio-temporal non-stationarity is particularly important for regional precipitation prediction tasks.

- Time dependence: The water content of clouds gradually changes over time, which effects on the precipitation at the next moment (Konapala et al., 2020). Moreover, the shorter the time interval, the stronger the temporal dependence

reflected by precipitation. As shown in Fig.1, which demonstrates the hourly precipitation at a site over time, it can be seen that the current precipitation is influenced by the past precipitation.

- Spatial dependence: The current precipitation is related not only to the local precipitation at previous moments, but also to the past precipitation in the surrounding area (Wu et al., 2019). As shown in Fig.2, due to the influence of wind, the precipitation zone moves hourly from northwest to southeast, eventually leaving Jiangsu Province.

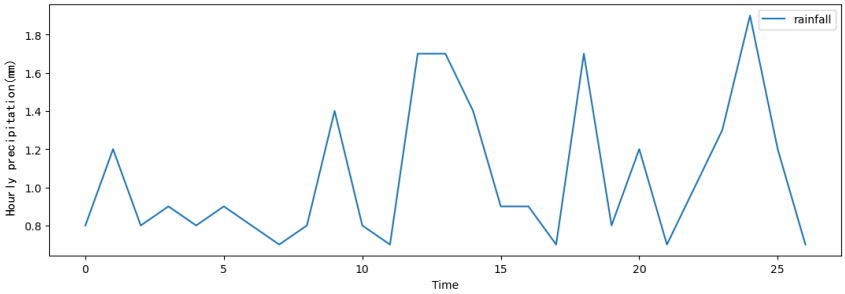

Figure 1. Hourly precipitation of one station (mm).

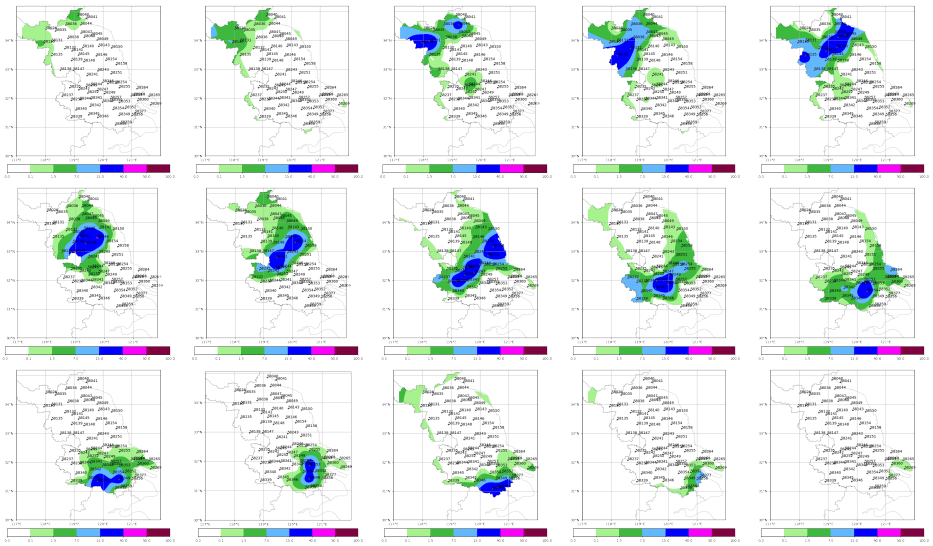

Figure 2. Location of precipitation zones in Jiangsu Province over time: July 6, 2019, 4:00–18:00.

There are many methods used for spatio-temporal forecasting in the field of computing, some of which consider temporal dependence, including the support vector regression machine model (Cai et al., 2018), the Kalman filter model (Nerini et al., 2019), the autoregressive integrated moving average (ARIMA) model (H. R. Wang et al., 2014), the K-nearest neighbor model (Huang et al., 2017) and Bayesian model (Ji et al., 2019) The above methods predict future data via histori-

cal data, only considering the dynamic changes in the data and ignoring the spatial dependence; as such, they cannot achieve satisfactory results if directly used for the prediction of regional short- term intense precipitation. A number of methods have been developed for describing the spatial characteristics by introducing convolutional neural networks(CNN) (Barra et al., 2020) (Ran et al., 2021) for spatial modeling. However, CNN is typically employed for Euclidean data (Defferrard et al., 2016), such as images and regular grids. This is incompatible with the distribution of automatic weather stations in both urban and rural regions, and hence is irrelevant to this problem.

To improve the accuracy and stability of precipitation forecasting, we propose a short-term regional precipitation prediction model based on wind-improved spatiotemporal convolutional network(ASS-TGCN) based on the data of national automatic stations.Our contribution is divided into the following three points:

- Meteorological data are processed to build a dataset for automatic stations in Jiangsu province. The adjacency matrix between stations based on distance and Pearson correlation coefficients is calculated to construct the topology and capture the spatial correlation.
- The ASS-TGCN model integrates the improved Graph Convolution Network (GCN) and Gated Recurrent Unit (GRU). The improved GCN is used to capture the spatial correlation modeling of the topological structure, taking into account the effects of the wind direction at past moments and geographical location; whilst GRU is used to capture the dynamics of the data in order to modele temporal correlation. The Spatiotemporal memory flow module and attention module are added to capture spatial deformation and temporal variation more accurately. Thus, the proposed model is more in line with the physical characteristics of precipitation and thus more suitable for precipitation prediction tasks that require higher accuracy of prediction.
- We applied the proposed model to the established dataset and conducted a series of comparison experiments with related models. On the self-built dataset, the experimental results show that the model improves the TS score by 0.14 and 0.19 points and reduces the MSE by about 16 and 22 points with respect to the GRAPES and T639, respectively, proving that the model has better performance for the precipitation prediction task.

The rest of the paper is organized as follows: Section II reviews the related studies on precipitation prediction; Section III presents the details of our model, including the creation of the dataset, the reasons for selecting the basic model and its improvement; Section IV evaluates the prediction performance of ASS-TGCN in real-world operations; and Section V presents some conclusions and recommendations for further study.

2 Related Work

In recent years, there are two main models for precipitation prediction(Zhang et al., 2017): Section 2.1 presents the traditional physical statistical model and Section 2.2 presents the data-driven model.

2.1 Physical statistical models

The main tool for current rainfall forecasting is the numerical weather prediction (NWP) model. The NWP models used in China are mainly the European Centre for Medium-Range Weather Forecasting (ECMWF) (Molteni et al., 1996), the Japan Meteorological Agency numerical weather prediction model (JAPAN) (Honda

et al., 2005), and the Global/Regional Assimilation Forecasting System (GRAPES) (D. Chen et al., 2008). The NWP model first analyzes the existing weather data to determine the degree of correlation between various weather attributes, and then processes them using relevant mathematical principles (Bauer et al., 2015). This process mainly includes the Kalman filter method (Yang, 2019)and, the regression analysis method (Hoolohan et al., 2018) (H. R. Wang et al., 2014), and eventually obtaining more accurate prediction formulas; thus, these physical statistical models have stringent data quality criteria. Since the NWP model uses various means (Powers et al., 2017) (conventional observations (Wahl et al., 2017), radar observations (Thomas et al., 2020), ship observations (Petty, 2020), satellite observations (Hagelin et al., 2021), etc.) to obtain meteorological data, they must be adjusted, processed, and objectively analyzed appropriately. Also, regional factors have a great impact on prediction accuracy (Xie et al., 2020). Since the computational data of NWP is so large, it is difficult to process by hand or with small computers (Xiaolong et al., 2019), therefore, a mainframe is necessary. However, due to the limitation of the whole discipline level, it is very difficult to accurately predict urban rainfall and its temporal and spatial distribution before the rainstorm. Therefore, In terms of actual application, these models are not flexible enough and vulnerable to the influence of unstable factors, and cannot stably predict rainfall in different regions.

2.2 Data-driven models

To overcome the aforementioned limitations, data-driven models have been utilized for precipitation forecasting. Such models use system state variables as input and output to establish the correspondence between state variables (Abouie et al., 2017).This kind of approach is more popular because it focuses more on characteristics between historical data. For example, (Seo & Kim, 2012) used support vector machine and KNN based on steady-state genetic algorithm to study the genetic feature selection method based on wrapper, which is used to predict very short-term rainstorm in the south of the Korean Peninsula. With the development of neural networks (Ghazvinian et al., 2020), many researchers have used Recurrent neural networks to implement prediction. However, due to the defects of Recurrent Neural Network (RNN), such as gradient disappearance and gradient explosion, the traditional RNN has limitations in long-term prediction(Fang et al., 2021). The GRU network (Che et al., 2018) is a variant of recurrent neural networks based on the long and short-term memory network (SHI et al., 2015) that has been shown to solve the above problems. Through the integration of forgetting gate and input gate in LSTM network and the change of cell state, it optimizes the overall structure of the network, so as to improve the network solution speed while retaining the advantages of LSTM network. The problems of long time dependence and gradient explosion are optimized. (Salehin et al., 2020) proposed an amount of rainfall prediction model with LSTM, which is applied to memory sequence data measurement and calculate the prediction result promptly. However, this kind of method only considers the historical information of the current location and ignores the spatial information, resulting in poor performance in practice. Many scholars have introduced convolutional neural networks (CNN) into their models(Yin et al., 2021)(L. Chen et al., 2020) to demonstrate spatial dependence of the precipitation. (Manokij et al., 2019) proposed a network combined of CNN and GRU to perform multi-step rainfall forecasting in Thailand, where CNN aims to capture relationship between various sensors and GRU aims to capture time-series information. (SHI et al., 2015) introduced convolution structure to improve the fully connected LSTM, proposed convolution LSTM (ConvLSTM) model for precipitation prediction. On this basis, Trajectory Gru (TrajGRU) model (Shi et al., 2017) is proposed, which can actively learn the position variation structure of recursive connection. Most of the above algorithms use CNN, which require radar echoes or satellite images as input, and

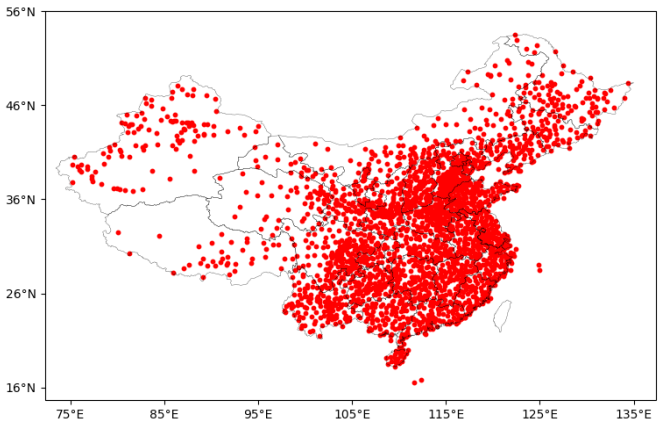

Figure 3. Distribution map of national meteorological automatic stations

these data are not easily available in remote mountainous or poor areas. Compared with CNN, the Graph Convolutional Networks(GCN) can process arbitrary graph structure data by using the property that convolution is essentially filtering on the frequency domain(Ni et al., 2021). At present, it has been widely used in traffic flow prediction(Zhao et al., 2019)(Bai et al., 2021), pedestrian prediction(Liu et al., 2021), wind speed prediction(Stańczyk & Mehrkanoon, 2021) and so on. GE-STDGN(Ni et al., 2021) proposed a graph structure learning algorithm and an optimization method based on evolutionary multi-objective optimization (EMO) algorithm to improve the ability of the model to analyze the correlation of complex nodes.

Considering that the distribution of automatic meteorological stations in China is consistent with the topological network of GCN, and they are widely used in China, as of July 31, 2020, 1,185 automatic meteorological stations have been established in poor townships across the country that are operational as scheduled (Zong et al., 2021), as shown in Fig.3. These weather stations can be used for all-weather on-site monitoring of wind speed, wind direction, rainfall, air temperature, air humidity, light intensity, evaporation, atmospheric pressure, and many other meteorological elements(Ioannou et al., 2021). The data obtained will be transmitted to the meteorological database for statistical analysis and processing, which is an important way to fill the gap of meteorological detection data on these areas. Therefore, we carry out short-term precipitation prediction tasks through an improved spatio-temporal convolution model based on automatic station data.

3 Data and Methodology

3.1 Construction of dataset

The initial data set was obtained from the National Automatic Station numerical files, covering a total of 16 months from June to September between 2016 and 2019. The process was as follows: First, according to the Chinese automatic station number table, all station numbers in Jiangsu Province were selected. Then, the initial file was read and the various meteorological data of the stations were extracted in the order of stations according to the filtered numbers, which were saved in csv format for subsequent reading and sorting. Then, we extracted the precipitation, hourly wind speed and wind direction data according to the field table, and saved

them as a month table in the order of station number and time. We found that the extracted precipitation data had some missing data; some of the data were missing for a single moment at some stations, and some were missing for all stations at a particular moment. Since we need continuous time-series data to capture the temporal dynamics of precipitation, we interpolated the missing data by referring to the data at the previous and next moments.

There are five kinds of precipitation data contained in the automatic station file: cumulative precipitation within the past 1 hour, 3 hours, 6 hours, 12 hours and 24 hours. Through comparison, it was found that 1-hour cumulative precipitation reflects a small amount of time-dependent characteristics, and can reflect a certain spatial distribution. Also, some temporal correlations can be seen from the 3-hour cumulative precipitation data. As the interval of time increases, the temporal correlation of the data increases and the spatial correlation decreases. Considering the timeliness of the forecast and the definition of short-term heavy precipitation, we eventually selected 1-hour cumulative precipitation as the raw data.

3.2 Construction of Adjacency Matrix

3.2.1 Correlation matrix based on distance

In order to generate the correlation matrix based on distance, we calculated the geographical distance between automatic weather station sensors according to longitude and latitude, and used Gaussian kernel with a threshold(Li et al., 2018).

$$W_{ij} = \exp\left(-\left(dist\left(v_i, v_j\right)^2\right)/\delta^2\right), \quad if\ dist\left(v_i, v_j\right) \leq k,\ otherwise\ 0. \tag{1}$$

where v_i, v_j are automatic weather stations; $dist$ is the geographical distance between v_i and v_j; δ is the standard deviation of the distance; W_{ij} is the edge weight between the stations; and k is the threshold.

3.2.2 Correlation matrix based on correlation of data

In order to represent the correlation of precipitation between several sites at the same time, we utilize the Pearson coefficient (Schober et al., 2018).

$$R\left(X,Y\right) = \frac{\sum_{i=1}^{n}\left(X_i - \bar{X}\right)\left(Y_i - \bar{Y}\right)}{\sqrt{\sum_{i=1}^{n}\left(X_i - \bar{X}\right)^2}\sqrt{\sum_{i=1}^{n}\left(Y_i - \bar{Y}\right)^2}}, \tag{2}$$

where $\bar{X}$ and $\bar{Y}$ represent the mean values of X and Y respectively. The range of $R\left(X,Y\right)$ is $[-1,1]$. When $R\left(x,y\right) = 1\ or\ -1$, it means that the two samples are completely related. When $R\left(x,y\right) = 0$, it means that the two samples are completely independent.

3.2.3 Constructing a new adjacency matrix

In line with the actual problem, the positive part of the matrix are isolated , and the rest are set to 0.

3.3 Improved spatiotemporal convolution network

(Zhao et al., 2019) presented a spatiotemporal forecasting model, Temporal Graph Convolutional Network (TGCN), for traffic flow forecasting. In light of the

fact that our task is comparable to traffic flow prediction in the following two aspects:

- Similar objectives: predict future values by analyzing the temporal and spatial relationship between the data of local and surrounding stations;
- Similar data composition: spatial relationship of multiple stations and their equal interval numerical data.

Therefore, we chose to make improvements on this model to make it more adequate for precipitation forecasting tasks.

3.3.1 Spatial dependence model

Due to the spatial dependence of rainfall, the precipitation in a region has a certain relationship with the surrounding areas. Therefore, obtaining complex spatial correlations is a key problem in precipitation prediction.

GCN is a first-order local approximation of spectral graph convolution, i.e., a multilayer graph convolutional neural network where each convolutional layer only deals with first-order neighborhood information. By superimposing several convolutional layers, GCN can achieve multi-order neighborhood information transfer in order to extract spatial features between nodes, defining the specific formula of the layer l in the convolutional network as follows:

$$H^{(l+1)} = \sigma\left(\widetilde{D}^{-\frac{1}{2}}\widetilde{A}\widetilde{D}^{-\frac{1}{2}}H^{(l)}W^{(l)}\right), \tag{3}$$

where $\widetilde{A} = A + I$ denotes the sum of the adjacency matrix A and the unit matrix I. Specifically, each vertex in the graph and itself plus an edge is able to learn the attribute features of its own nodes when the model is learned. $\widetilde{D}$ denotes the degree matrix of the adjacency matrix $\widetilde{A}$, which can be specifically expressed as $\widetilde{D}_{ii} = \sum_j \widetilde{A}_{ij}$. $H^{(l)}$ denotes the output of the layer l. when $l = 0$, H_0 equals the X-feature matrix, and $W^{(l)}$ is the parameter matrix of the layer l. σ denotes the sigmoid activation function of the nonlinear model. Generally, a GCN model can be expressed as follows:

$$f(X, A) = \sigma\left(\tilde{A}XW^{l}\right), \tag{4}$$

$$\hat{A}=\tilde{D}^{-\frac{1}{2}}\tilde{A}\tilde{D}^{-\frac{1}{2}}, \tag{5}$$

where $\tilde{A}$ denotes the symmetric normalization of the Laplace matrix, $\tilde{X}$ denotes the feature matrix composed of the data of each node, $\tilde{W}$ denotes the parameter matrix of the layer l of the neural network, $\tilde{H}$ denotes the number of hidden units, and $f(X, A)$ denotes the output data of each observation predicting the length of t.

3.3.2 Time dependence model

Since rainfall is time-series correlated over a short period of time, obtaining complex temporal correlations is another key issue in precipitation prediction. GRU network has significant advantages in sequence modeling and is often used to solve time series prediction problems. Through the integration of forgetting gate and input gate in LSTM network and the change of cell state, the GRU model optimizes the overall structure of the network, so as to improve the network solution speed while retaining the advantages of LSTM network. GRU model includes two door control units: update door and reset door. It is calculated as follows:

$$z_t = \sigma\left(W_z \cdot [h_{t-1}, x_t]\right), \tag{6}$$

$$r_t = \sigma\left(W_r \cdot [h_{t-1}, x_t]\right), \tag{7}$$

$$\tilde{h}_t = \tanh\left(W \cdot [r_t * h_{t-1}, x_t]\right), \tag{8}$$

$$h_t = (1 - z_t) * h_{t-1} + z_t * \tilde{h}_t, \tag{9}$$

where z_t and r_t are the outputs of the update and reset gates respectively; σ denotes the sigmoid activation function; W_z and W_r are the weight coefficient matrices of the update and reset gates respectively, obtained from the model training; h_{t-1} is the state information of the previous time step in the GRU neural network; x_t is the input of the current time step. $\tilde{h}_t$ and h_t are the pre-output is the output and output, respectively, of time step t.

3.3.3 Improved GCN model

In the traditional GCN, since the graph is undirected, the adjacency matrix is a symmetric matrix; that is $A_{ij} = A_{ji}$, as in Fig.4. In the precipitation problem, which is affected by the wind direction, the interactions between sites are different, as in Fig.5. Under the influence of the northeast wind, the precipitation at site i will affect site j, while the precipitation at site j will not affect site i; that is $A_{ij} > 0$ and $A_{ji} = 0$, so $A_{ij} \neq A_{ji}$.

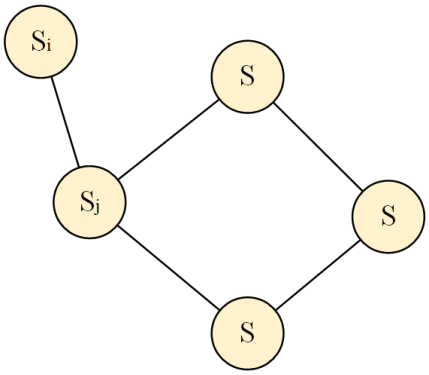

Figure 4. General GCN node relationship

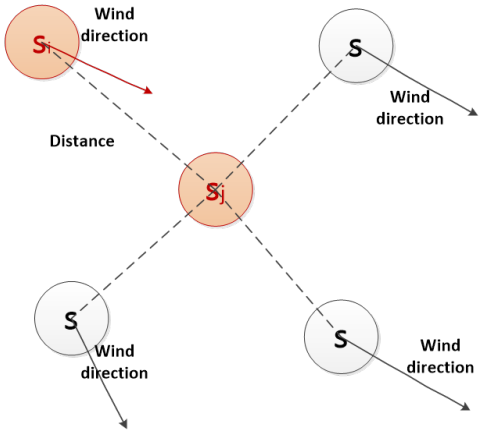

Figure 5. Node relationship affected by wind direction in precipitation problem

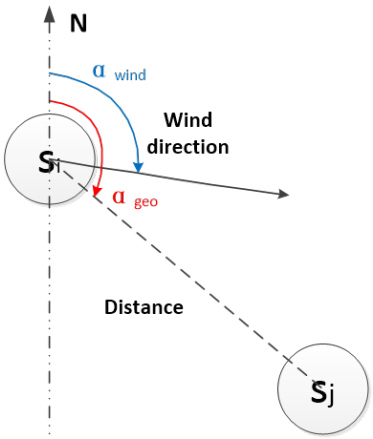

Figure 6. Impact of site i on site j

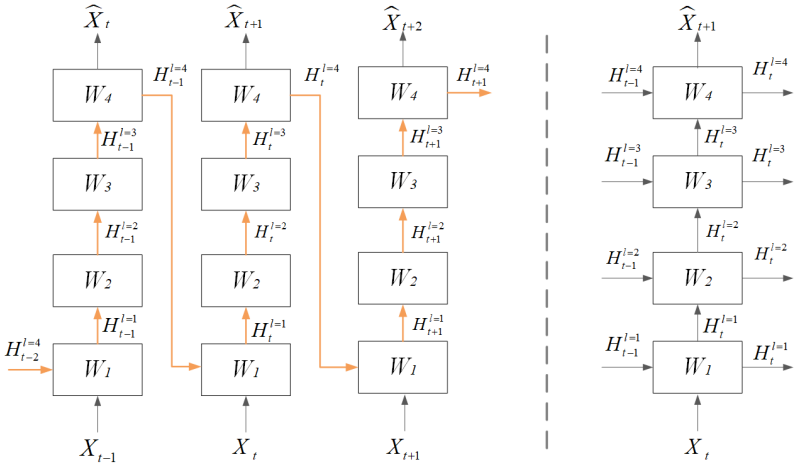

Figure 7. Left: GRU network model with spatiotemporal memory(Y. Wang et al., 2017), right: traditional GRU model

Therefore, as shown in Fig.6, we define the influence of wind direction on site i and site j at a certain time as follows:

$$R_{ij} = cos\left(\alpha_{wind} - \alpha_{geo}\right) \tag{10}$$

The influence of distance between site i and site j is:

$$W_{ij} = exp\left(-\frac{dist\left(s_i - s_j\right)}{\delta^2}\right) \tag{11}$$

Therefore,

$$\widetilde{A}_{ij} = FC\left(R_{ij}\right) + FC\left(W_{ij}\right) + I \tag{12}$$

$$f(X, A) = \sigma\left(\widehat{A} ReLU\left(\widehat{A} X W_0\right) W_1\right) \tag{13}$$

where $\widehat{A} = \widetilde{D}^{-\frac{1}{2}} \widetilde{A} \widetilde{D}^{-\frac{1}{2}}$ denotes the preprocessing step, W_0 and W_1 denote the weights. $f(X, A)$ represents the output of prediction length t and $ReLU()$ represents the rectified linear unit.

3.3.4 Improved spatiotemporal convolution network combined with wind direction

To capture the spatial and temporal characteristics of precipitation data, we propose an improved spatiotemporal convolution network combined with GCN and GRU, and consider the influence of wind direction on the results (ASS-TGCN), as shown in Fig.8:

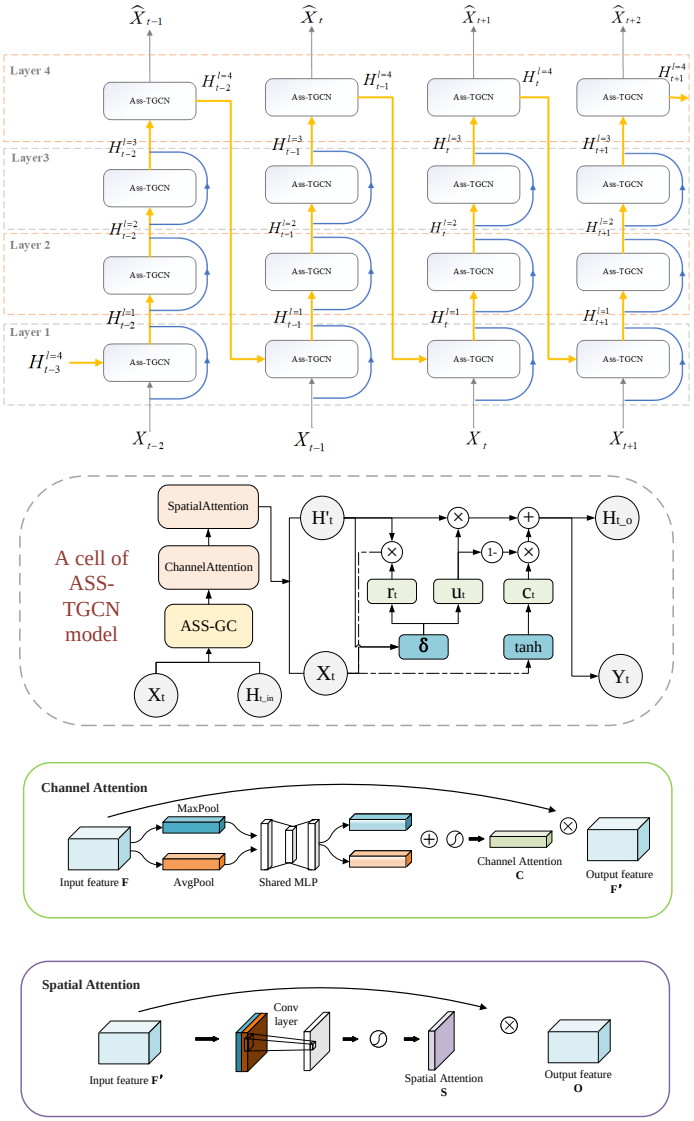

Figure 8. Improved residual spatiotemporal convolution network

The specific calculation process is as follows: $f(X, A)$ represents the result after ASS-GCN processing, W and b represent the weights and biases, respectively, at training.

$$u_t^{l=1} = \delta\left(W_u \cdot \left[h_{t-1}^{l=4}, f\left(A, x_t\right)\right] + b_u\right) \tag{14}$$

$$r_t^{l=1} = \delta\left(W_r \cdot \left[h_{t-1}^{l=4}, f\left(A, x_t\right)\right] + b_r\right) \quad (15)$$
$$c_t^{l=1} = \tanh\left(W_c \cdot \left[r_t^{l=1} * h_{t-1}^{l=4}, f\left(A, x_t\right)\right] + b_c\right) \quad (16)$$
$$h_t^{l=1} = u_t^l * h_{t-1}^{l=4} + \left(1 - u_t^l\right) * c_t^l \quad (17)$$
$$u_t^{l\neq 1} = \delta\left(W_u \cdot \left[h_t^{l-1}, f\left(A, \left(x_t + h_t^{l-1}\right)\right)\right] + b_u\right) \quad (18)$$
$$r_t^{l\neq 1} = \delta\left(W_r \cdot \left[h_t^{l-1}, f\left(A, \left(x_t + h_t^{l-1}\right)\right)\right] + b_r\right) \quad (19)$$
$$c_t^{l\neq 1} = \tanh\left(W_c \cdot \left[r_t^l * h_t^{l-1}, f\left(A, \left(x_t + h_t^{l-1}\right)\right)\right] + b_c\right) \quad (20)$$
$$h_t^{l\neq 1} = u_t^l * h_t^{l-1} + \left(1 - u_t^l\right) * c_t^l \quad (21)$$

In summary, the proposed model can handle complex spatial dependencies and temporal dynamics. On the one hand, the improved GCN is used to learn the complex topology in order to capture the spatial dependencies based on distance and wind direction, and GRU is used to learn the dynamic changes in the data in order the data to capture the temporal dependencies. The temporal memory flow module and attention module are added to capture spatial deformation and temporal variation more accurately. The residual module makes the network with short connections more capable of fitting high-dimensional functions than the network with normal connections.

4 Experiments and discussions

4.1 Data introduction

4.1.1 Meteorological element data

Considering the original data set, the 1-hour cumulative precipitation is of more practical significance, and the wind direction with 1-hour extreme wind speed can better reflect the impact of wind direction on regional short-term precipitation. Therefore, to serve as the original dataset, we selected the hourly precipitation and the wind direction of 1-hour extreme wind speed of 67 automatic stations in Jiangsu Province (excluding three remote stations) from June to September between 2016 and 2019. The data interval is 1 hour, for a total of 9720 $\times$ 67 respectively. To address data loss and distortion caused by missing measurements and failures of automatic stations, the following process was performed: First, we remove the points with values of 99999 and 99990 (representing missing and omitted measurements). Then we use the isolated forest algorithm to filter out the abnormal points. Finally, we use the method of linear interpolation to assign values to all missing values.

There are many moments in this dataset with almost no precipitation over the whole Jiangsu province; therefore, we further processed the dataset in order to avoid biased fitting of the network predictions in the direction of no precipitation. Following (Trebing et al., 2021), we select samples with more than 20% of the total number of stations with precipitation at each moment on average. Although the number of filtered samples is much smaller than the initial data set, they are more suitable for regional precipitation forecasting. (SHI et al., 2015) did something similar by selecting the first 97 rainy days for training in their 3-year dataset. Furthermore, due to the nature of rainfall maps where rainfall dominates, the model may be biased towards predicting more rainfall. In the experiment, the input data is normalized to the interval [0,1]. 80% of the data is set as the training dataset, whilst the remaining 20% serves as the test dataset. In this way, we use the past 12 hours of precipitation and wind direction as the historical data to predict the next 3-hours of precipitation.

4.1.2 Adjacency matrix data

From the original data, we filtered out 67 station numbers in Jiangsu province, extracted the latitude and longitude of the stations based on the numbers, and used them to build a distance matrix. Then we calculate the correlation between stations based on the correlation between precipitation at the same time at different stations in the training set. Finally, in line with the actual problem, we isolated the positive part of the data correlation matrix and the distance correlation matrix, and set the other parts to 0. In this way, we obtained the required adjacency matrix.

4.2 Evaluation metrics

We use the following four metrics to evaluate the performance of different forecasting models:

4.2.1 Mean Squared Error (MSE)

$$MSE = \frac{1}{MN}\sum_{j=1}^{M}\sum_{i=1}^{N}\left(y_i^j - \hat{y}_i^j\right)^2, \tag{22}$$

4.2.2 Mean Absolute Error (MAE)

$$MAE = \frac{1}{MN}\sum_{j=1}^{M}\sum_{i=1}^{N}\left|y_i^j - \hat{y}_i^j\right|, \tag{23}$$

4.2.3 Threat Score (TS)

$$TS = \frac{(TP+TN)}{(TN+FP+FN+TP)}, \tag{24}$$

MSE and MAE are used to provide a measure of forecast error: the smaller the value, the better the prediction result. TS(Wang & Chung-Chieh, 2014) is a quantitative test of forecast accuracy and is used to detect the degree of forecast accuracy for precipitation greater than a certain level: the larger the value, the better the prediction result.

4.3 Model parameter setting

To train the model, we had to select appropriate model parameters for the experiments. The hyperparameters in the ASS-TGCN model include learning rate, batch size, number of training epochs, and number of hidden units. We set the learning rate to 0.008, the batch size to 50, and the training epochs to 100. The number of hidden units in the ASS-TGCN model is an important parameter which has a significant impact on prediction accuracy. To determine the optimal value, we set the number of hidden units to 8,16,32,64,128 to test and analyze the prediction results by comparing MSE values, as shown in Fig.9 Through this process, the best number of hidden units was determined to be 64.

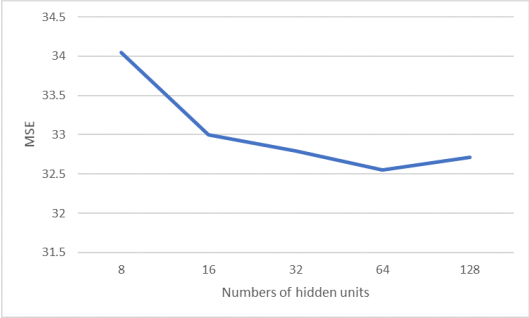

Figure 9. Comparison of prediction performance with different numbers of hidden units

4.4 Experimental results

First, we compared the 3-hour cumulative precipitation values predicted by the following models: GCN(Verma et al., 2018), GRU(Che et al., 2018), and T-GCN(Zhao et al., 2019).

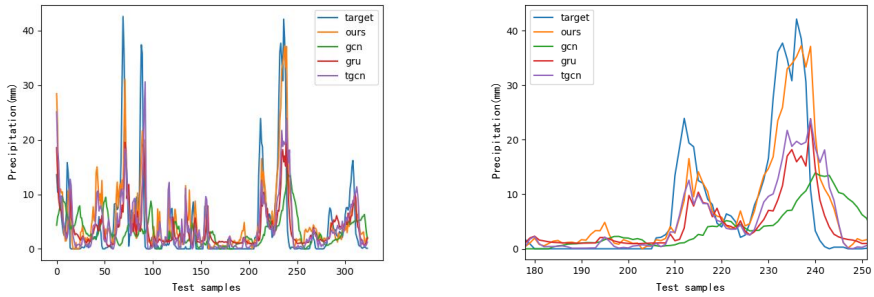

Figure 10. Forecast results of 3-hour cumulative precipitation using different models:ground truth (blue), GCN forecasts (green), GRU forecasts (red), TGCN forecasts (purple), ASS-TGCN forecasts (orange). The left figure shows the results of all test samples, and the right figure shows the results (enlarged) of samples No.180 to No.250).

Table1 shows the prediction of the proposed model and other models on the cumulative precipitation in the next three hours. It can be seen from the table that the MSE and MAE values of GCN and GRU are high, and those of the other two models are similar to each other. Most models exhibit good accuracy under the indicators of TS_0.1 and TS_1.5, but GCN and GRU perform poorly on TS_3.0, TS_7.0 and TS_10.0. Only TS_15.0 and TS_20.0 of the proposed model are greater than 0.1, and the rest are less than 0.01. Thus the proposed model has good performance according to most evaluation metrics, especially in long-term medium and high-grade precipitation.

From the comparison between the predicted value and the real value of a single site, GCN produces poor results in a single site because it does not take into

Table 1. Comparison of 3-hour cumulative precipitation forecast values for each model.

NO. 58037									
	MSE	MAE	TS_0.1	TS_1.5	TS_3.0	TS_7.0	TS_10.0	TS_15.0	TS_20.0
GCN	64.344	4.645	0.668	0.472	0.333	0.084	0.042	0.000	0.000
GRU	40.383	3.575	0.660	0.562	0.544	0.370	0.313	0.276	0.000
TGCN	38.473	3.473	0.664	0.607	0.536	0.408	0.373	0.257	0.050
ASS-TGCN	**29.222**	**3.162**	**0.671**	**0.600**	**0.541**	**0.526**	**0.483**	**0.389**	**0.348**
All									
	MSE	MAE	TS_0.1	TS_1.5	TS_3.0	TS_7.0	TS_10.0	TS_15.0	TS_20.0
GCN	52.574	3.963	0.545	0.368	0.285	0.115	0.058	0.000	0.000
GRU	38.706	3.270	0.543	0.473	0.335	0.266	0.266	0.133	0.049
TGCN	33.727	2.949	**0.580**	**0.543**	0.514	0.418	0.348	0.212	0.088
ASS-TGCN	**32.548**	**2.929**	0.569	0.535	**0.515**	**0.432**	**0.359**	**0.259**	**0.162**

account the time correlation. The trend of the predicted value of GRU is consistent with the real value, but there is a serious timing delay because only the time correlation is considered. T-GCN comprehensively considers the correlation between time and space, and exhibits certain optimization in peak value and timing delay compared with the first two algorithms. ASS-TGCN considers the influence of past wind direction and geographical location on the basis of T-GCN. The spatiotemporal memory flow module and attention module make the spatial deformation and temporal change captured by the network more accurate, and the residual module increases the fitting ability to high-dimensional functions. Therefore, the prediction result is closest to the real value, and the timing delay is the smallest. Overall, it produces the best prediction of 3-hour cumulative precipitation values.

Fig.11 shows the mean distribution of MSE of different models on the test set. Blue indicates small MSE and red indicates large MSE. It can be seen that for all models, the error is mainly concentrated in the southwest of Jiangsu, but the error level of the proposed model is obviously better than other models. We suspect that the reason is that the precipitation here is affected by the water vapor generated by the Yangtze River in the north and Taihu Lake in the southeast; in addition, the model only uses the precipitation of the station as the data input (although the proposed model introduces the wind direction as a reference), which can not solve this problem completely. Compared with TGCN, the proposed model has smaller MSE and more uniform overall error distribution for stations around latitude 32.7°N, reflecting the advantages of the model.

Fig.12 shows that given the same batch size and learning rate, ASS-TGCN can master the law of precipitation zone movement faster during the learning process because it considers more geographical and practical information. Therefore, compared with other models, ASS-TGCN exhibits faster convergence speed and can reach the optimal value faster.

Next, we compared the predictions of the proposed model with two numerical weather prediction models.

- T639_L60(Zheng et al., 2019): T639_L60 global medium range numerical prediction model possesses high model resolution, reaching a global horizontal resolution of 30 km, a vertical resolution of 60 layers, and a model upper limit of 0.1 HPA. In addition, this model produces a higher vertical resolution of

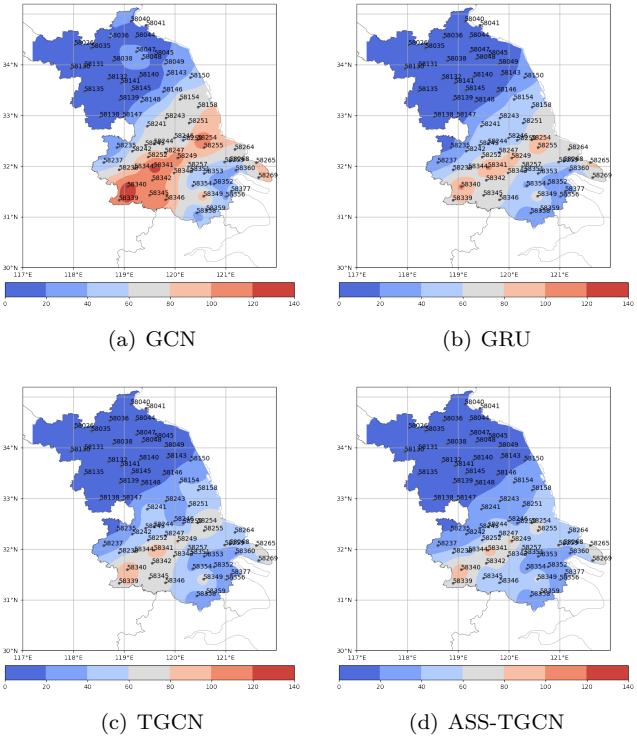

(a) GCN (b) GRU

(c) TGCN (d) ASS-TGCN

Figure 11. Distribution of MSE of different models on the test set

boundary layers and a more detailed description of boundary layer process, which is more suitable for supporting short-term proximity prediction. After comparison in operational practice, it is considered that the prediction accuracy of basic elements such as H, T, and P of the situation field of T639 is improved. The operational application of T639 global medium range numerical forecast assimilation forecast system has greatly improved the weather forecasting capability in China, with increased forecast.

- GRAPES_MESO (Liping et al., 2017): The GRAPES_MESO model has shown good forecasting performance for precipitation. To investigate the correctness and effectiveness of the GRAPES system, a series of standard tests and application simulations have been conducted, including the application of conventional data analysis together with direct analysis of radar and satellite unconventional data. The system has been operated in national and regional meteorological operation centers, and has played an important role in actual meteorological operations. The model has certain forecasting capability for strong weather processes such as heavy precipitation; in particular, the high spatial and temporal resolution products can better describe the development of the process to a certain extent.

Table2 shows the prediction of the proposed model and two numerical models for the 3-hour cumulative precipitation. It can be seen that ASS-TGCN and TGCN perform similarly in the terms of MSE and MAE, for both optimal and suboptimal values. GRAPES and T639 perform well on the low-level TS score (TS_0.1, TS_2.5 and TS_3.0), GRAPES and ASS-TGCN performis similarly on the middle-level TS score(TS_7.0 and TS_10.0), and ASS-TGCN achieves the best performance in the high-level TS score(TS_15.0 and TS_20.0). Thus, the proposed model performs well in medium and high grade precipitation. Compared with NWP models, the low-level

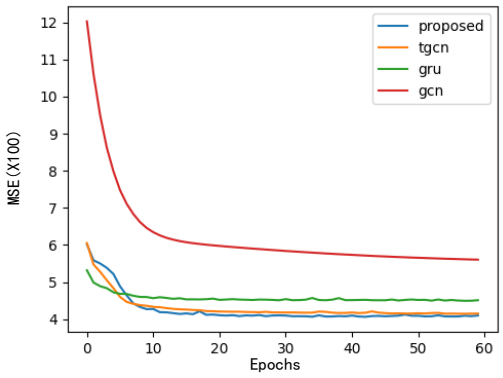

Figure 12. Convergence speed of different models

Table 2. Comparison of 3-hour cumulative precipitation forecast values with two NWP models

	MSE	MAE	TS_0.1	TS_1.5	TS_3.0	TS_7.0	TS_10.0	TS_15.0	TS_20.0
GRAPE	39.118	3.081	**0.758**	**0.717**	**0.610**	0.508	0.482	0.423	0.227
ASS-TGCN	**23.446**	2.698	0.617	0.598	0.586	**0.596**	**0.584**	**0.434**	**0.362**
GCN	51.087	3.921	0.600	0.449	0.326	0.199	0.114	0.000	0.000
GRU	27.849	2.931	0.593	0.574	0.510	0.484	0.489	0.254	0.073
TGCN	23.856	**2.569**	0.617	0.592	0.583	0.565	0.575	0.361	0.214
	MSE	MAE	TS_0.1	TS_1.5	TS_3.0	TS_7.0	TS_10.0	TS_15.0	TS_20.0
T639	44.991	3.314	**0.654**	0.434	0.349	0.076	0.049	0.041	0.014
ASS-TGCN	**22.794**	2.539	0.608	**0.591**	**0.537**	**0.455**	**0.427**	**0.323**	**0.228**
GCN	41.474	3.477	0.578	0.448	0.355	0.178	0.063	0.000	0.000
GRU	28.733	2.874	0.579	0.564	0.529	0.393	0.314	0.130	0.038
TGCN	23.121	**2.427**	0.627	0.636	0.547	0.449	0.406	0.278	0.054

TS score is close, the medium and high-level TS score is better, and the MSE is significantly improved; Compared with other models, TS score is generally better and MSE is close to the best.

Fig.13-14 show prediction results from the NWP models and the proposed model at different time points of large-scale medium-grade precipitation in Jiangsu Province. As can be seen from figures, compared with other models, the precipitation zone predicted by the proposed model is closer to the real one, demonstrating certain prediction ability for medium-and-high-intensity precipitation.

Fig.15-16 show the actual error between the predicted value and the real value of each model in Fig.13-14. Blue indicates the part where the predicted value is less than the real value and red indicates the part where the predicted value is greater than the real value; the darker the color is, the greater the difference is. It can be seen that in Fig.15, the predicted values of GCN and GRU in central Jiangsu is relatively small, whilst the predicted values of TGCN and GRAPES in southern Jiangsu are relatively large. Compared with the above models, the error of the proposed model over the whole Jiangsu Province is relatively small and the error distribution is relatively average; In Fig.16, almost all models have low predicted values in the area of latitude 32 °N to 33 °N, and the precipitation at station No.58269 has not

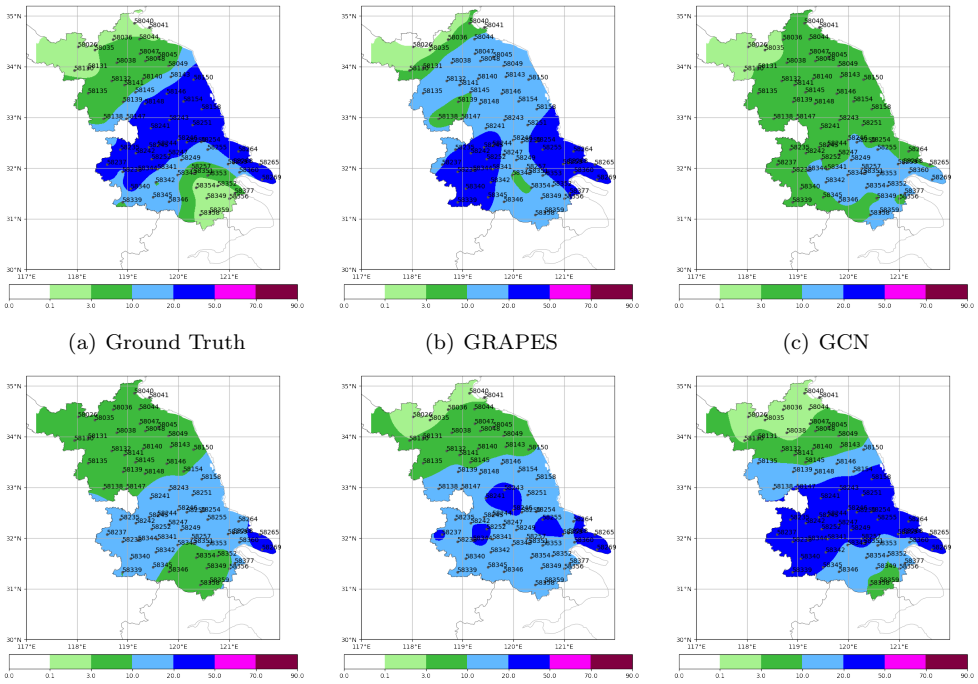

(a) Ground Truth (b) GRAPES (c) GCN

(d) GRU (e) TGCN (f) ASS-TGCN

Figure 13. Comparison of forecast results with GRAPES at 2016/09/16 0:00-3:00

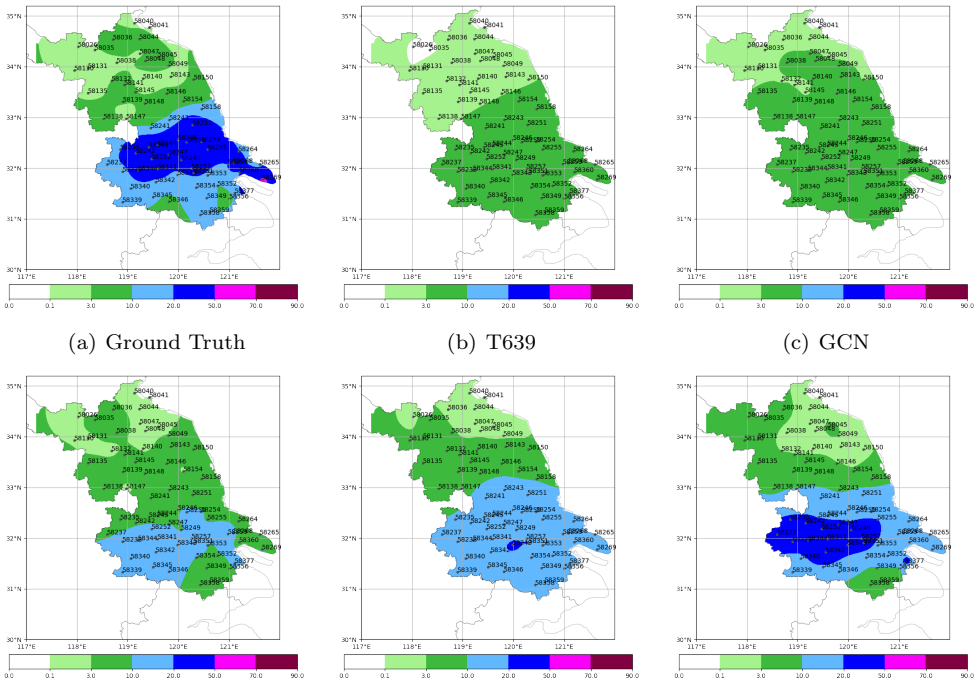

(a) Ground Truth (b) T639 (c) GCN

(d) GRU (e) TGCN (f) ASS-TGCN

Figure 14. Comparison of forecast results with T639 at 2016/09/15 20:00-23:00

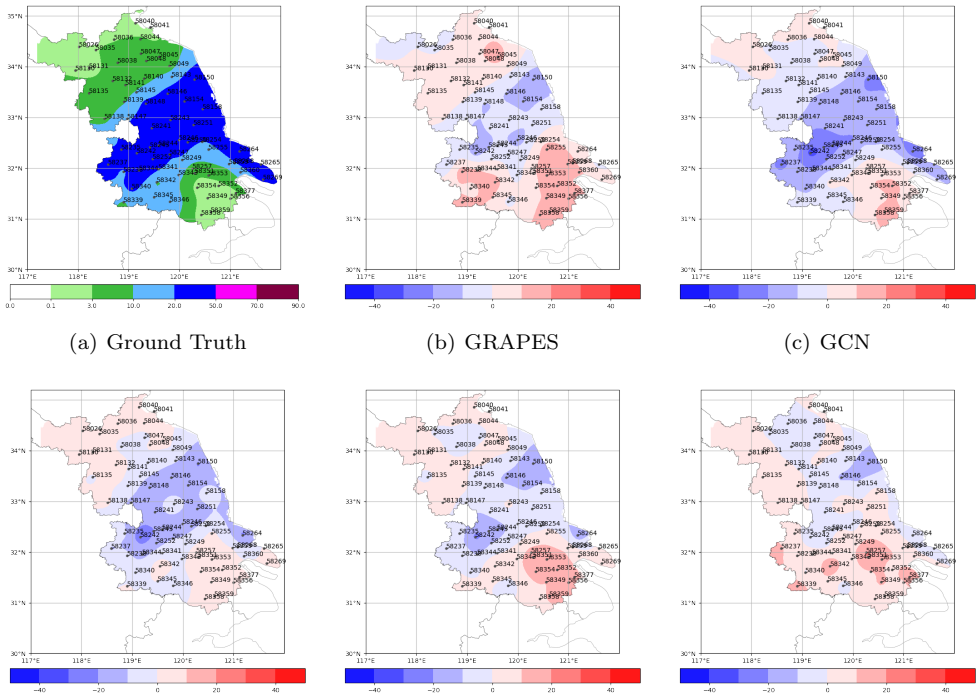

(a) Ground Truth (b) GRAPES (c) GCN

(d) GRU (e) TGCN (f) ASS-TGCN

Figure 15. The actual error between the predicted value and the real value of each model in Fig.13

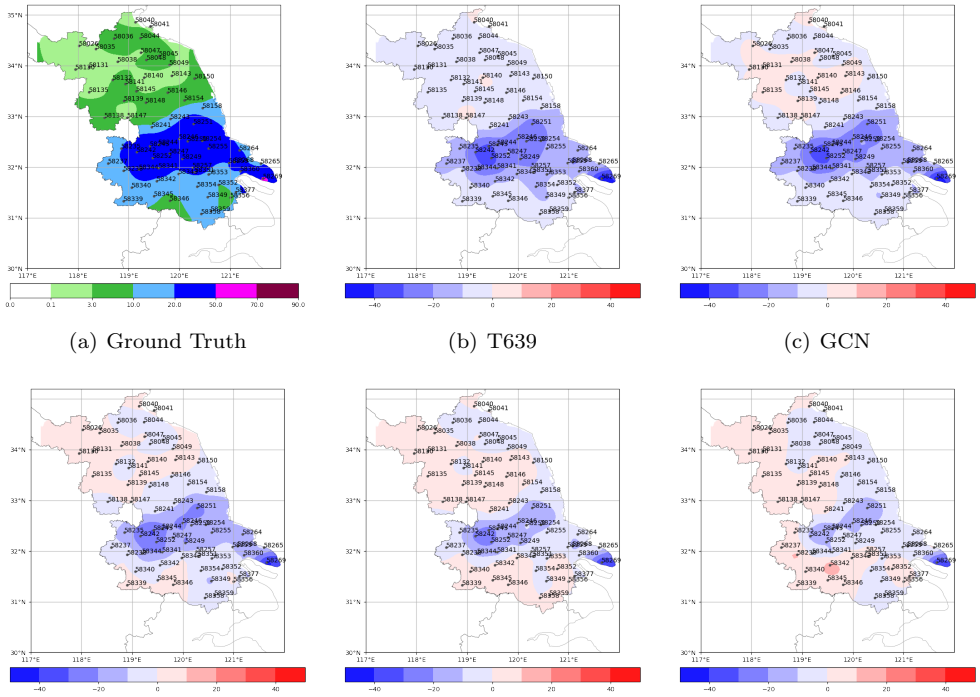

(a) Ground Truth (b) T639 (c) GCN

(d) GRU (e) TGCN (f) ASS-TGCN

Figure 16. The actual error between the predicted value and the real value of each model in Fig.14

been accurately predicted. It can also be seen that the proposed model demonstrates a lower error level and more uniform error distribution.

5 Conclusion

In this paper, a short-term regional precipitation prediction model based on wind-improved spatiotemporal convolutional network is proposed. Among them, the improved GCN comprehensively considers the influence of past wind direction and geographical location in order to capture spatial dependence; whilst GRU is used to learn the dynamic changes in the data in order to capture time dependence. Spatio-temporal memory flow module and attention module are added to more accurately capture spatial deformation and temporal changes, thereby better matching the physical properties of precipitation. According to the results of a series of experiments, the proposed model can handle complex spatial dependence and temporal dynamic changes, understand the temporal and spatial characteristics of precipitation data, and achieve better prediction results.

For further study, we will incorporate more meteorological elements into the model as a priori knowledge, so that the model can better learn the impact of different meteorological elements at different distances and times on the future precipitation at the current station, improve the prediction accuracy of extreme values, and realize end-to-end grid.

6 Open Research

The data of the automatic weather station is provided by the Beijing Meteorological Bureau and is required to be kept confidential. However, the hourly observation data of China's surface meteorological stations can also be downloaded from: http://data.cma.cn/data/cdcdetail/dataCode/A.0012.0001.html

Acknowledgments

This work is granted by National Natural Science Foundation of China(61773220) and Key program of National Natural Science Foundation of China(U20B2061).

References

Abouie, A., Darabi, H., & Sepehrnoori, K. (2017). Data-driven comparison between solid model and pc-saft for modeling asphaltene precipitation. *Journal of Natural Gas Science and Engineering*, *45*, 325–337.

Bai, J., Zhu, J., Song, Y., Zhao, L., Hou, Z., Du, R., & Li, H. (2021). A3t-gcn: Attention temporal graph convolutional network for traffic forecasting. *ISPRS International Journal of Geo-Information*, *10*(7), 485.

Ban, N., Schmidli, J., & SchäR, C. (2015). Heavy precipitation in a changing climate: Does short-term summer precipitation increase faster? *Geophysical Research Letters*, *42*(4), 1165-1172.

Barra, S., Carta, S. M., Corriga, A., Podda, A. S., & Recupero, D. R. (2020). Deep learning and time series-to-image encoding for financial forecasting. *IEEE/CAA Journal of Automatica Sinica*, *7*(3), 683-692.

Bauer, P., Thorpe, A., & Brunet, G. (2015). The quiet revolution of numerical weather prediction. *Nature*, *525*(7567), 47–55.

Cai, C., Wang, J., & Li, Z. (2018). Improving tigge precipitation forecasts using an svr ensemble approach in the huaihe river basin. *Advances in Meteorology*, *2018*, 1-16.

Che, Z., Purushotham, S., Cho, K., Sontag, D., & Liu, Y. (2018). Recurrent neural networks for multivariate time series with missing values. *Scientific reports*, *8*(1), 1–12.

Chen, D., Xue, J., Yang, X., Zhang, H., Shen, X., Hu, J., ... Chen, J. (2008). New generation of multi-scale nwp system (grapes): general scientific design. *Chinese Science Bulletin*, *53*(22), 3433–3445.

Chen, L., Cao, Y., Ma, L., & Zhang, J. (2020). A deep learning-based methodology for precipitation nowcasting with radar. *Earth and Space Science*, *7*(2), e2019EA000812.

Defferrard, M., Bresson, X., & Vandergheynst, P. (2016). Convolutional neural networks on graphs with fast localized spectral filtering. *Advances in neural information processing systems*, *29*, 3844–3852.

Fang, W., Chen, Y., & Xue, Q. (2021). Survey on research of rnn-based spatio-temporal sequence prediction algorithms. *Journal on Big Data*, *3*(3), 97.

Ghazvinian, H., Bahrami, H., Ghazvinian, H., & Heddam, S. (2020). Simulation of monthly precipitation in semnan city using ann artificial intelligence model. *Journal of Soft Computing in Civil Engineering*, *4*(4), 36–46.

Hagelin, S., Azad, R., Lindskog, M., Schyberg, H., & Körnich, H. (2021). Evaluating the use of aeolus satellite observations in the regional numerical weather prediction (nwp) model harmonie–arome. *Atmospheric Measurement Techniques*, *14*(9), 5925–5938.

Hawkins, E., & Sutton, R. (2011). The potential to narrow uncertainty in projections of regional precipitation change. *Climate Dynamics*, *37*(1-2), 407-418.

Henderson, J., Nielsen, E. R., Herman, G. R., & Schumacher, R. S. (2020). A hazard multiple: Overlapping tornado and flash flood warnings in a national

weather service forecast office in the southeastern united states. *Weather and Forecasting*, *35*(4), 1459–1481.

Honda, Y., Nishijima, M., Koizumi, K., Ohta, Y., Tamiya, K., Kawabata, T., & Tsuyuki, T. (2005). A pre-operational variational data assimilation system for a non-hydrostatic model at the japan meteorological agency: Formulation and preliminary results. *Quarterly Journal of the Royal Meteorological Society: A journal of the atmospheric sciences, applied meteorology and physical oceanography*, *131*(613), 3465–3475.

Hoolohan, V., Tomlin, A. S., & Cockerill, T. (2018). Improved near surface wind speed predictions using gaussian process regression combined with numerical weather predictions and observed meteorological data. *Renewable Energy*, *126*, 1043–1054.

Huang, M., Lin, R., Huang, S., & Xing, T. (2017). A novel approach for precipitation forecast via improved k-nearest neighbor algorithm. *Advanced Engineering Informatics*, *33*, 89–95.

Ioannou, K., Karampatzakis, D., Amanatidis, P., Aggelopoulos, V., & Karmiris, I. (2021). Low-cost automatic weather stations in the internet of things. *Information*, *12*(4), 146.

Ji, L., Zhi, X., Zhu, S., & Fraedrich, K. (2019). Probabilistic precipitation forecasting over east asia using bayesian model averaging. *Weather and Forecasting*, *34*(2), 377–392.

Konapala, G., Mishra, A. K., Wada, Y., & Mann, M. E. (2020). Climate change will affect global water availability through compounding changes in seasonal precipitation and evaporation. *Nature communications*, *11*(1), 1–10.

Li, Y., Yu, R., Shahabi, C., & Liu, Y. (2018). Diffusion convolutional recurrent neural network: Data-driven traffic forecasting. In *International conference on learning representations* (p. 1-16).

Liping, H., Dehui, C., Liantang, D., Zhifang, X., Fei, Y., Yuan, J., & Feifei, Z. (2017). Main technical improvements of grapes_meso v4. 0 and verification. *Journal of Applied Meteorological Science*, *28*(1), 25–37.

Liu, M., Li, L., Li, Q., Bai, Y., & Hu, C. (2021). Pedestrian flow prediction in open public places using graph convolutional network. *ISPRS International Journal of Geo-Information*, *10*(7), 455.

Manokij, F., Sarinnapakorn, K., & Vateekul, P. (2019). Forecasting thailand's precipitation with cascading model of cnn and gru. In *2019 11th international conference on information technology and electrical engineering (icitee)* (p. 1-6). doi: 10.1109/ICITEED.2019.8929975

Molteni, F., Buizza, R., Palmer, T. N., & Petroliagis, T. (1996). The ecmwf ensemble prediction system: Methodology and validation. *Quarterly journal of the royal meteorological society*, *122*(529), 73–119.

Nerini, D., Foresti, L., Leuenberger, D., Robert, S., & Germann, U. (2019). A reduced-space ensemble kalman filter approach for flow-dependent integration of radar extrapolation nowcasts and nwp precipitation ensembles. *Monthly Weather Review*, *147*(3), 987–1006.

Ni, Q., Wang, Y., & Fang, Y. (2021). Ge-stdgn: a novel spatio-temporal weather prediction model based on graph evolution. *Applied Intelligence*, 1–15.

Petty, G. (2020). Trends in ship-reported oceanic precipitation frequency from 1958 through 2014. *Earth and Space Science Open Archive ESSOAr*, 20.

Powers, J. G., Klemp, J. B., Skamarock, W. C., Davis, C. A., Dudhia, J., Gill, D. O., ... others (2017). The weather research and forecasting model: Overview, system efforts, and future directions. *Bulletin of the American Meteorological Society*, *98*(8), 1717–1737.

Ran, Y., Wang, H., Tian, L., Wu, J., & Li, X. (2021). Precipitation cloud identification based on faster-rcnn for doppler weather radar. *EURASIP Journal on Wireless Communications and Networking*, *2021*(1), 1-20.

Salehin, I., Talha, I. M., Hasan, M. M., Dip, S. T., Saifuzzaman, M., & Moon, N. N. (2020). An artificial intelligence based rainfall prediction using lstm and neural network. In *2020 ieee international women in engineering (wie) conference on electrical and computer engineering (wiecon-ece)* (pp. 5–8).

Schober, P., Boer, C., & Schwarte, L. A. (2018). Correlation coefficients: appropriate use and interpretation. *Anesthesia & Analgesia*, *126*(5), 1763–1768.

Seo, J.-H., & Kim, Y.-H. (2012). Genetic feature selection for very short-term heavy rainfall prediction. In *International conference on hybrid information technology* (pp. 312–322).

SHI, X., Chen, Z., Wang, H., Yeung, D.-Y., Wong, W.-k., & WOO, W.-c. (2015). Convolutional lstm network: A machine learning approach for precipitation nowcasting. In *Advances in neural information processing systems* (Vol. 28, p. 1-9).

Shi, X., Gao, Z., Lausen, L., Wang, H., Yeung, D.-Y., Wong, W.-k., & Woo, W.-c. (2017). Deep learning for precipitation nowcasting: A benchmark and a new model. *Advances in neural information processing systems*, *30*.

Stańczyk, T., & Mehrkanoon, S. (2021). Deep graph convolutional networks for wind speed prediction. *arXiv preprint arXiv:2101.10041*.

Thomas, G., Mahfouf, J.-F., & Montmerle, T. (2020). Toward a variational assimilation of polarimetric radar observations in a convective-scale numerical weather prediction (nwp) model. *Atmospheric Measurement Techniques*, *13*(5), 2279–2298.

Trebing, K., Stańczyk, T., & Mehrkanoon, S. (2021). Smaat-unet: Precipitation nowcasting using a small attention-unet architecture. *Pattern Recognition Letters*, *145*, 178–186.

Verma, N., Boyer, E., & Verbeek, J. (2018). Feastnet: Feature-steered graph convolutions for 3d shape analysis. In *Proceedings of the ieee conference on computer vision and pattern recognition* (pp. 2598–2606).

Wahl, S., Bollmeyer, C., Crewell, S., Figura, C., Friederichs, P., Hense, A., ... Ohlwein, C. (2017). A novel convective-scale regional reanalysis cosmo-rea2: Improving the representation of precipitation. *Meteorologische Zeitschrift*, *26*(4), 345-361.

Wang, & Chung-Chieh. (2014). On the calculation and correction of equitable threat score for model quantitative precipitation forecasts for small verification areas: The example of taiwan. *Weather & Forecasting*, *29*(4), 788-798.

Wang, H. R., Wang, C., Lin, X., & Kang, J. (2014). An improved arima model for precipitation simulations. *Nonlinear Processes in Geophysics,21,6(2014-12-01)*, *21*(6), 1159-1168.

Wang, Y., Long, M., Wang, J., Gao, Z., & Yu, P. S. (2017). Predrnn: Recurrent neural networks for predictive learning using spatiotemporal lstms. *Advances in neural information processing systems*, *30*, 1-10.

Wu, P., Ding, Y., Liu, Y., & Li, X. (2019). The characteristics of moisture recycling and its impact on regional precipitation against the background of climate warming over northwest china. *International Journal of Climatology*, *39*(14), 5241–5255.

Xiaolong, H., Bin, D., & Wei, W. (2019). Comparative analysis of the observation data of automatic precipitation weather phenomenon instrument. In *2019 international conference on meteorology observations (icmo)* (p. 1-4). doi: 10.1109/ICMO49322.2019.9025841

Xie, P., Joyce, R., Wu, S., Ren, L., & Katz, B. (2020). Monitoring heavy precipitation with the cmorph integrated satellite precipitation estimates. In *Igarss 2020 - 2020 ieee international geoscience and remote sensing symposium* (p. 3309-3312). doi: 10.1109/IGARSS39084.2020.9324229

Yang, D. (2019). On post-processing day-ahead nwp forecasts using kalman filtering. *Solar Energy*, *182*, 179–181.

Yao, S., Chen, H., & Han, L. (2021). Short-term prediction of precipitation associated with landfalling hurricanes through deep learning. In *2021 ieee international geoscience and remote sensing symposium igarss* (p. 7176-7179). doi: 10 .1109/IGARSS47720.2021.9553303

Yin, J., Gao, Z., & Han, W. (2021). Application of a radar echo extrapolation-based deep learning method in strong convection nowcasting. *Earth and Space Science*, *8*(8), e2020EA001621.

Zhang, P., Jia, Y., Gao, J., Song, W., & Leung, H. (2018). Short-term rainfall forecasting using multi-layer perceptron. *IEEE Transactions on Big Data*, *6*(1), 93–106.

Zhang, P., Zhang, L., Leung, H., & Wang, J. (2017). A deep-learning based precipitation forecasting approach using multiple environmental factors. In *2017 ieee international congress on big data (bigdata congress)* (pp. 193–200).

Zhao, L., Song, Y., Zhang, C., Liu, Y., Wang, P., Lin, T., ... Li, H. (2019). T-gcn: A temporal graph convolutional network for traffic prediction. *IEEE Transactions on Intelligent Transportation Systems*, *21*(9), 3848–3858.

Zheng, J., Gao, L., & Ren, H. (2019). Verification of china extreme temperature forecasts in 2016 based on t639 ensemble forecast. *Meteorological Monthly*, *45*(4), 469-482.

Zong, L., Liu, S., Yang, Y., Ren, G., Yu, M., Zhang, Y., & Li, Y. (2021). Synergistic influence of local climate zones and wind speeds on urban heat island and heat waves in beijing. *Frontiers in Earth Science*, *9*, 458.